

## High-contrast, high-resolution focusing of neutral atoms using light forces

Vasant Natarajan, Robert E. Behringer, and Gregory Timp  
 AT&T Bell Laboratories, Murray Hill, New Jersey 07974

(Received 3 May 1995)

We show that light force lenses can be used to focus a thermal beam of neutral atoms with extremely high resolution ( $\sim 20$  nm) and high contrast ( $\sim 10:1$ ), finally making such atom-optical lenses viable for proposed applications. Our (cylindrical) lenses for sodium atoms are created by the dipole force within each period of a standing wave. We determine the spatial distribution of the focused atoms (with nanometer resolution) by allowing the atoms to deposit on a substrate and scanning with a UHV scanning tunneling microscope. We find that the requirements for optimum focusing are very large, positive detuning; short focal lengths; and a well-collimated atomic beam. These dependences can be thoroughly understood from a simple theoretical model. [S1050-2947(96)07306-4]

PACS number(s): 42.50.Vk, 32.80.-t, 42.82.Cr, 03.75.Be

The recent growth in understanding of atom-photon interactions has led to the demonstration of several atom-optical elements, such as atom lenses and atom mirrors, using light forces [1]. The fine control of neutral atom beams promised by such techniques could have tremendous impact in atom interferometry and other proposed applications such as lithography [2,3], high-resolution surface microprobes [4], and spatially controlled crystal growth. However, this projected impact depends on demonstrating high-quality elements for realistic atom beams, something that has not been achieved heretofore. For example, a high-quality lens should have good contrast and high resolution, but all the focusing experiments thus far have suffered from poor contrast. In fact, when the contrast is poor and not well understood, it is inappropriate to even measure the lens resolution. Our goal, therefore, has been to understand light focusing in order to develop a high-quality atom-optical lens.

In this paper, we demonstrate such a lens for a thermal sodium beam using a nearly resonant standing-wave (SW) laser beam. Under optimal conditions, we achieve an unprecedented focal width of 20 nm with a contrast of about 10:1. Our success has been the result of three main developments. First, we had to extend a theoretical model to understand focusing under realistic conditions. Only then were we able to understand the various lens aberrations and design an optimum lens for a thermal atom beam. Second, we had to obtain high-contrast focusing, without which it was impossible to reliably interpret the dependence of resolution on experimental lens parameters. Finally, we had to measure the spatial distribution of focused atoms with high resolution. We have achieved this with an *in situ* ultrahigh vacuum (UHV) scanning tunneling microscope (STM). We allow the focused atoms to deposit on a substrate before imaging with the STM. This has given us the unprecedented ability to accurately measure the atomic distribution under different focusing conditions with a resolution of about 5 nm.

Our experimental setup is shown schematically in Fig. 1. The sodium source is maintained at 420 °C in an UHV chamber ( $\sim 10^{-10}$  Torr). It produces a beam of atoms with an (estimated) rms velocity of 860 m/s and a transverse collimation of about 3 mrad near the SW interaction region. The collimation is further improved using one-dimensional mo-

lasses cooling [5] below the SW. The silicon substrate (typically  $6 \times 6$  mm<sup>2</sup>) is clamped rigidly with respect to a mirror used to retroreflect the incoming SW and molasses beams. This ensures that there is no variation in the spatial phase of the SW during deposition. The substrate intersects the SW beam near the intensity maximum and the atoms deposit after the interaction with negligible free flight.

All the laser beams are derived from a dye laser that is offset locked to the  $3S_{1/2}$ ,  $F=2 \rightarrow 3P_{3/2}$ ,  $F'=2$  sodium transition (589 nm) in a separate absorption cell using FM Doppler-free spectroscopy. The SW and molasses beams are both measured to have approximately Gaussian profiles. The beam waists are located at the retro-mirror with typical  $1/e^2$  diameters of 100  $\mu\text{m}$  and 1 cm, respectively.

For each deposition, we use a clean silicon sample with a hydrogen passivated surface [6]. The hydrogen is desorbed in UHV by heating the silicon to 550 °C. The *in situ* heating is crucial for obtaining metallic sodium deposition and making good STM imaging contact [7]. The focused atoms form a grating on the silicon surface, which diffracts in the visible spectrum. The diffraction efficiency gives us a reliable estimate of the fidelity of the grating over the sample, which is useful since the STM image only covers an area of 1  $\mu\text{m}^2$  at a time. The sample is transferred to the STM chamber while

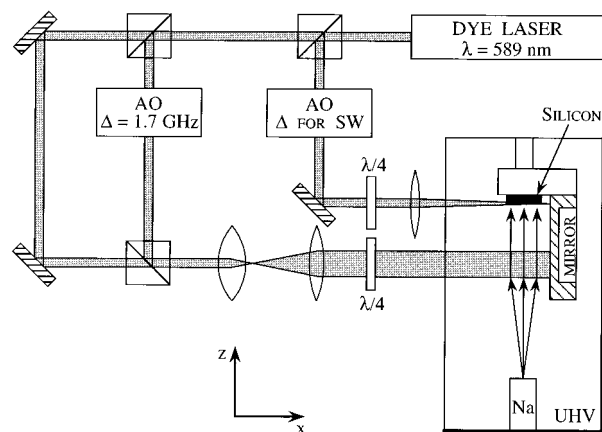


FIG. 1. Schematic of the experiment.

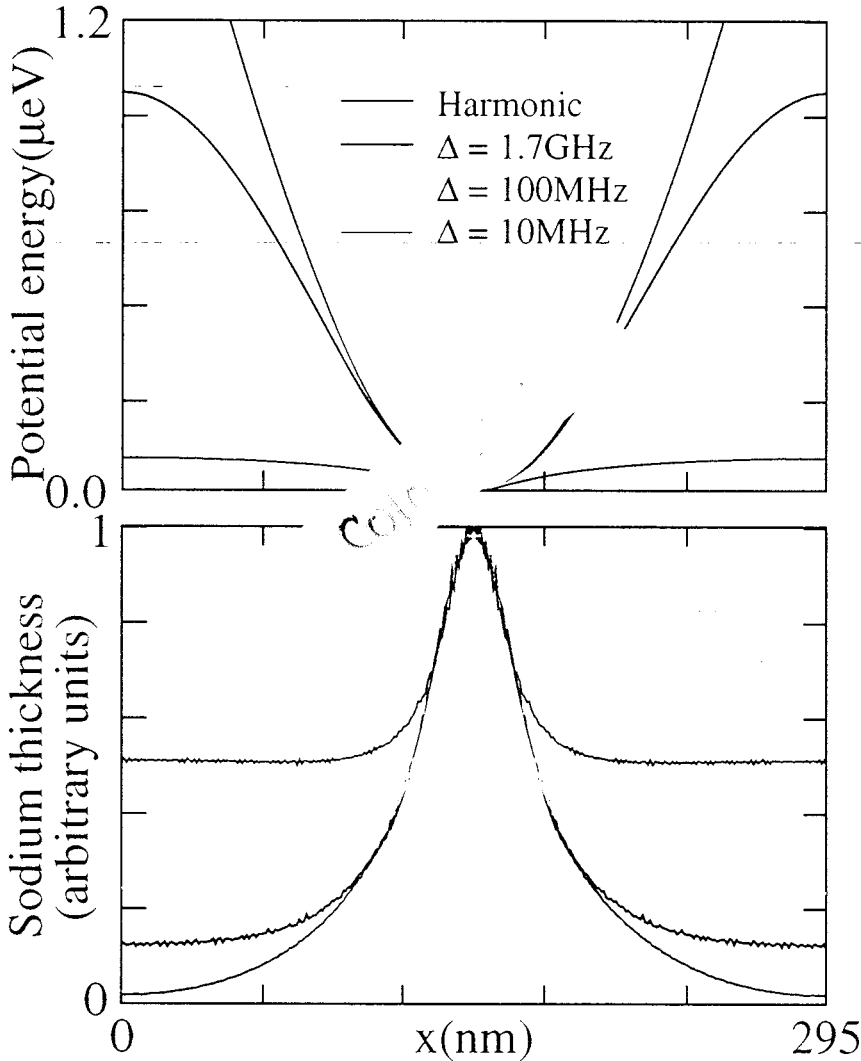


FIG. 2. Effect of potential shape. The optical potential within one period of the SW depends on  $\Delta$ , shown in the upper part for  $\Delta = +10, 100$ , and  $1700$  MHz. The intensity at each detuning is adjusted so that the oscillation time near the bottom of the well (harmonic region) is the same. Also shown for comparison is a perfectly harmonic potential. The predicted atomic distribution after focusing in these four potentials is shown below from semiclassical numerical simulations corresponding to the detunings above. Note the progressive degradation of contrast at lower detunings.

in UHV and can be imaged cleanly for a few hours (at  $\leq 10^{-9}$  Torr) before surface degradation begins to cause some instability in the scans.

We now consider the details of the focusing process in order to design the optimal atom lens for a thermal atom beam. In the simplest model, the sodium atom can be treated as a two-level system. We use the sodium  $D_2$  line at  $589.0$  nm; in particular, most of our studies have used the strongest transition from the  $3S_{1/2}$ ,  $F=2$ ,  $m_F=2$  ground state to the  $3P_{3/2}$ ,  $F'=3$ ,  $m_{F'}=3$  excited state coupled using  $\sigma^+$  light. The optical dipole force due to light nearly resonant with such a transition has been derived previously [8,9]. Since we operate in a transient regime, where the atom interacts with the light only for a short duration as it traverses the SW, the form of this force depends on the interaction time and the spontaneous scattering rate. The scattering rate is equal to  $p\Gamma$ , where  $p$  is the saturation parameter given by

$$p = \frac{I}{I_0} \frac{1}{1 + 4\Delta^2/\Gamma^2}, \quad (1)$$

where  $I$  is the laser intensity,  $I_0$  ( $=6.29$  mW/cm<sup>2</sup>) is the saturation intensity for the particular transition,  $\Delta$  is the detuning from the transition, and  $\Gamma$  ( $=10$  MHz) is the line-

width of the excited state. If the atom undergoes several spontaneous emissions during the interaction, the average force is obtained from the potential [8]

$$U = \frac{\hbar\Delta}{2} \ln(1+p). \quad (2)$$

On the other hand, if the atom undergoes no spontaneous emissions, the potential becomes coherent and takes the form [9]

$$U = \frac{\hbar\Delta}{2} \sqrt{1+2p}. \quad (3)$$

This is called the dressed-state potential. The atom preferentially projects into one of the two dressed states when it enters the SW and, without spontaneous emission, remains in that state for the duration of the interaction. From Eq. (1), this condition is satisfied at large detunings.

In both cases, the potential depends on the intensity through the saturation parameter  $p$ . We use the intensity variation within each period of the SW to provide the force needed to focus the atoms traversing it. In an ideal situation, an atom from a perfectly collimated, monochromatic beam

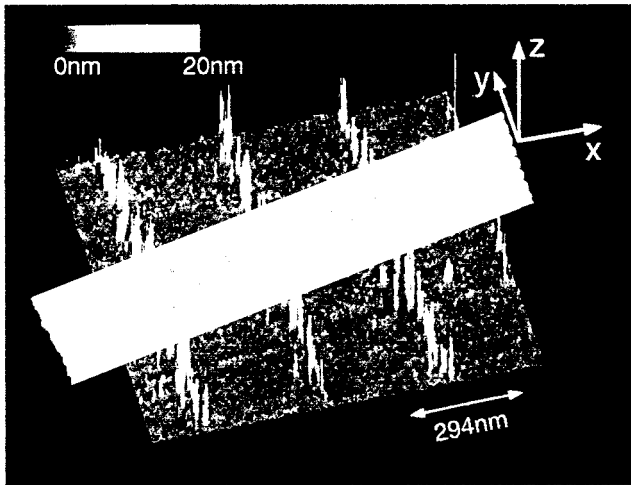


FIG. 3. STM micrograph of sodium deposited on silicon. The sodium distribution was obtained from a 35-s deposition under optimal focusing conditions in the SW:  $\Delta = +1710$  MHz,  $w_0 = 56$   $\mu\text{m}$ , and there is a power of 8 mW in each traveling wave. The molasses beam parameters were  $\Delta = -12$  MHz,  $w_0 = 5$  mm, and there is an input power of 50 mW in a lin  $\perp$  lin configuration. The resultant linewidth is about 20 nm and the contrast is about 10:1.

enters a period of the SW with equal probability across the  $\lambda/2$  potential well. Assuming that the well is perfectly harmonic, the atom has an oscillation period  $T$  independent of its amplitude (entry point in the well). Therefore, after a time

$T/4$ , all the atoms are at the bottom of the well and the beam is perfectly focused.

Within this model, we can now understand how the parameters of the atom beam affect the focal width and contrast. First, in order to be influenced by the potential and be focused, the atoms must enter the light field in the correct ( $F=2$ ) ground state. We achieve this in the molasses cooling region. The cooling light (which, as in the SW, drives the  $F=2 \rightarrow F'=3$  transition) has mixed into it light exactly resonant with the  $F=1 \rightarrow F'=2$  transition. This serves the dual purpose of pushing the thermal population of  $F=1$  ground-state atoms into the  $F=2$  ground state and preventing optical pumping into the  $F=1$  ground state during the cooling cycles. Next, the interaction time in the SW determines how well we satisfy the  $T/4$  timing condition. It depends on the longitudinal velocity of the atoms and the length of the light field. Since we use a thermal beam, we have a range of longitudinal velocities and, for each velocity, the focal point is slightly different. This is analogous to the effect of chromatic aberrations when focusing white light. Finally, the collimation of the atom beam determines the initial transverse velocity with which atoms enter the potential well. With a finite initial velocity, a given atom reaches the bottom of the potential at a time different from  $T/4$ . This has an adverse effect on spot size much as collimation does in ray optics.

We now turn to the effect of the SW parameters on the

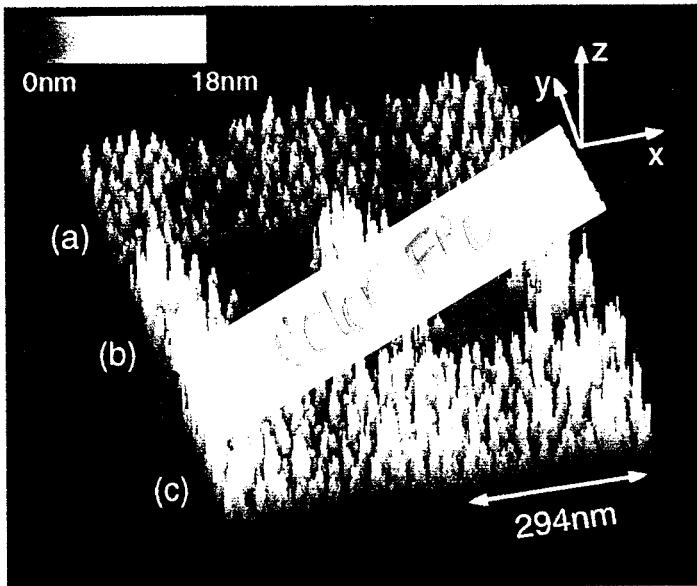
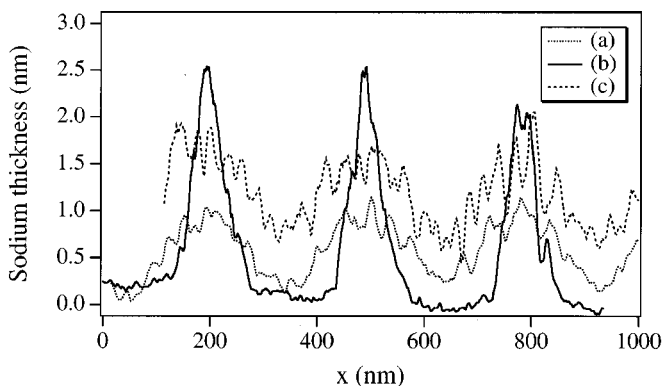


FIG. 4. Effect of different parameters on sodium focusing. The beam was collimated with ordinary Doppler molasses in (a) and (b), using  $\Delta = -5$  MHz,  $w_0 = 5$  mm, and an input power of 7.5 mW ( $\sigma$  polarized). In (a) the SW interaction length was increased by a factor of 4 ( $w_0 = 224$   $\mu\text{m}$ ), in (b) the SW conditions were identical to that of Fig. 3, and in (c) the molasses cooling beam was turned off to degrade the atom beam collimation by a factor of 6. The dramatic degradation in linewidth in (a) and both linewidth and contrast in (c) are clear from the average line profiles shown below. The poor focusing in (c) actually required us to run for 50% longer in order to get sufficient image contrast, hence the overall increase in area under the curve.



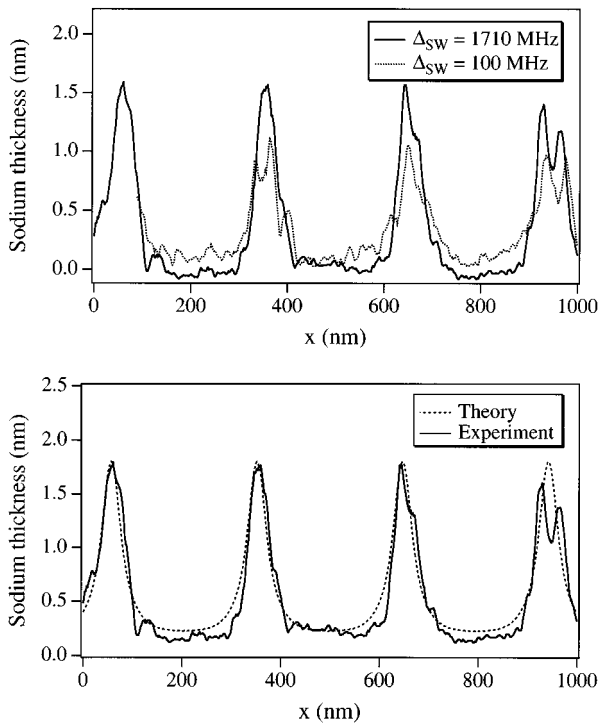


FIG. 5. Effect of detuning. The profiles in the upper figure represent sodium distributions obtained at the two detunings under the same focusing conditions as in Fig. 4(b), but with the input power at 100 MHz scaled to 700  $\mu$ W to match the timing condition. The lower figure shows a comparison between theory and experiment at 1.7 GHz. The prediction from theory under these conditions has already been considered in Fig. 2.

lens performance. To begin with, we want the potential to be as harmonic as possible since anharmonic terms degrade the atom lens just as spherical aberrations in an optical lens. For this, positive  $\Delta$  is better than negative  $\Delta$ . With  $\Delta > 0$ , the atoms are attracted to the nodes of the SW and the expansion of the potential is around small values of  $p$ . Second, for a fixed oscillation period ( $T$ ) near the bottom of the well, the value of  $p$  required is smaller at larger detunings and therefore the potential is more harmonic (see the inset of Fig. 2). For  $\Delta > 0$ ,  $T$  varies as  $1/\sqrt{p_0\Delta}$ , where  $p = p_0 \cos^2 kx$  in the SW; however, since  $I$  varies as  $p_0\Delta^2$  [Eq. (1)], the intensity (hence power) required to match the timing condition increases linearly with  $\Delta$ . Therefore, large, positive detunings result in a more harmonic potential, but require higher power to focus the atoms. Finally, the potential is deeper at higher detunings. This can be important since the atoms are only affected by a potential deeper than their initial transverse kinetic energy.

The results of these considerations are illustrated in Fig. 2. In the top part, we show the shapes of the potentials at different detunings, highlighting the increase in anharmonic terms and decrease in depth as we approach zero detuning. The effect of this on the focusing is seen from the resultant spatial distribution of atoms obtained from semiclassical numerical simulations given in the bottom of the figure [10]. At low detunings, there is a severe degradation of contrast because atoms entering the well in the anharmonic region away from the center are not properly focused. But near the well center, where the harmonic terms dominate, the line shape is

largely unaffected. This illustrates clearly the need to understand and measure contrast before the lens resolution can be addressed. If we were to simply measure the linewidth above background, we would erroneously conclude that smaller detunings result in higher resolution and that a harmonic potential gives the poorest resolution.

The interaction length in the light field (or the focal length of our effective lens) is also important in determining the linewidth. For a given beam divergence, the lens is equivalently imaging a finite-sized object from a finite distance. We then expect a shorter focal length lens to give lower magnification and thus a smaller image size. To understand this in the time domain, we note that a smaller interaction length requires a smaller oscillation time  $T$  (since the longitudinal velocity of the atoms getting focused is constant). Thus the transverse velocity acquired by the atoms when they reach the bottom of the well is larger and the effect of the initial velocity is less severe.

To summarize, the above analysis indicates that we can obtain narrowly focused lines with good atomic beam collimation; large, positive detunings; and a small interaction length. Since we use a Gaussian beam to form the SW and the substrate is located near the intensity maximum (beam center), the interaction length is directly related to the beam waist diameter  $w_0$ . Then, for different interaction lengths, we bring a given velocity group into focus by keeping  $w_0/T$  constant. From the dependence of  $T$  on  $I$ , we thus require constant  $Iw_0^2$ , i.e., constant power in the incoming beam [11]. To get different interaction lengths, we focus the same power down to different waist sizes. The detuning we choose is limited only by the power we can obtain at that frequency.

The experimental results support the general features of the analysis presented above. In Fig. 3, we show a STM micrograph of sodium distribution under optimal focusing conditions. The polarization gradient cooling used in the molasses results in a transverse temperature of about 25  $\mu$ K. The SW beam had a confocal parameter of 1.3 cm, which is the smallest we can use given the 5-mm distance from the sample to the mirror. The sodium grain size from this 35-s deposition is about 6 nm near the line center. The full width at half maximum of the line is 20 nm and the interline contrast is about 10:1; in fact, the roughness of the region between the lines is the same as that of a bare silicon surface, indicating that there is very little sodium present. The high contrast we obtain is partly due to good state preparation. With insufficient repumping light in the molasses beam, a significant fraction of the atoms exit the cooling region in the  $F=1$  ground state, forming a uniform background of unfocused atoms.

The importance of collimation and interaction length is shown in Fig. 4. The detuning and power in the SW were similar to those for Fig. 3. In Figs. 4(a) and 4(b), the beam was collimated using ordinary Doppler molasses cooling, which resulted in a transverse temperature of about 250  $\mu$ K, while in Fig. 4(c) the cooling was completely turned off. The roughly linear degradation with both collimation and interaction length is evident from the average line profiles across the three STM images shown in the lower portion of Fig. 4 (the silicon surface roughness of 0.8

nm has been subtracted from the averages to make the high contrast clear). Note that the STM image in Fig. 4(b) is also worse than the focusing shown in Fig. 3 obtained under nearly identical conditions, but where we used polarization gradient cooling to improve the collimation.

The dependence on SW detuning, seen from the line profiles in Fig. 5, is consistent with our expectations from Fig. 2. At  $\Delta=100$  MHz, the focusing is poorer with the contrast being noticeably degraded. As indicated by the simulations, the larger anharmonic content is primarily responsible for this effect. The depth of the potential at this detuning ( $\sim 4$  mK) is not a factor when the molasses cooling is on. However, it does become significant when the cooling is turned off (which makes the transverse temperature  $\sim 12$  mK): we do not observe any focusing under the conditions in Fig. 4(c) when  $\Delta=100$  MHz.

In Fig. 5, we also show the excellent agreement between the experimental line shape at  $\Delta=1.7$  GHz and the theoretical prediction shown in Fig. 2. We have done detailed numerical simulations to check the validity of our model over a wide range of experimental parameters [12] and this agree-

ment is quite typical [12]. It reflects our thorough understanding of the focusing process.

We have also studied the focusing as a function of intensity. We see only a 20% variation in linewidth over a range of a factor of 2. This is partly due to the thermal longitudinal velocity spread, which guarantees that some velocity group meets the  $T/4$  condition over this intensity range. It also indicates that chromatic aberrations are not very important at these focal widths.

In conclusion, we have shown that a well-collimated beam of neutral atoms can be focused to a spot size of 20 nm, even though the longitudinal velocity has a thermal spread. Using a theoretical model, we predict and experimentally confirm that the focal width is limited by the divergence of the atom beam and the length of the light interaction region. We should be able to increase the resolution below 10 nm by decreasing the interaction length to 20  $\mu\text{m}$ .

We would like to thank Jabez McClelland and Don Tennant for useful discussions.

- 
- [1] See, e.g., special issue on *Optics and Interferometry with Atoms*, edited by J. Mlynek, V. Balykin, and P. Meystre [Appl. Phys. B **54**, 321–481 (1992)].
- [2] G. Timp *et al.*, Phys. Rev. Lett. **69**, 1636 (1992).
- [3] J. J. McClelland, R. E. Scholten, E. C. Palm, and R. J. Celotta, Science **262**, 877 (1993).
- [4] T. Sleator, T. Pfau, V. Balykin, and J. Mlynek, Appl. Phys. B **54**, 375 (1992).
- [5] See special issue on *Laser Cooling and Trapping of Atoms*, edited by Steven Chu and Carl Wieman [J. Opt. Soc. Am. B **6**, 2020–2078 (1989)].
- [6] G. G. Higashi, Y. J. Chabal, G. W. Trucks, and K. Raghavachari, Appl. Phys. Lett. **56**, 656 (1990).
- [7] R. E. Behringer, V. Natarajan, and G. Timp, Appl. Surf. Sci. (to be published).
- [8] J. P. Gordon and A. Ashkin, Phys. Rev. A **21**, 1606 (1980).
- [9] J. Dalibard and C. Cohen-Tannoudji, J. Opt. Soc. Am. B **2**, 1707 (1985).
- [10] K. K. Berggren, M. Prentiss, G. L. Timp, and R. E. Behringer, J. Opt. Soc. Am. B **11**, 1166 (1994).
- [11] J. J. McClelland (private communication).
- [12] V. Natarajan, R. E. Behringer, D. M. Tennant, and G. Timp, J. Vac. Sci. Technol. B **13**, 2823 (1995).